

Supporting Information

Mitochondria-Targeted Zirconium Metal-Organic Frameworks for Enhancing Microwave Thermal Therapy Against Tumor

Hongqiao Zhou^a, Changhui Fu^b, Xiaowei Chen^c, Longfei Tan^b, Jie Yu^d, Qiong Wu^b, Liuhui Su^a, Zhongbing Huang^{*a}, Feng Cao^d, Xiangling Ren^b, Jun Ren^b, Ping Liang^{*d}, and Xianwei Meng^{*b}

^a College of Materials Science & Engineering, Sichuan University, Chengdu 610065, China.

E-mail addresses: zbhuang@scu.edu.cn

^b Laboratory of Controllable Preparation and Application of Nanomaterials, CAS Key Laboratory of Cryogenics, Technical Institute of Physics and Chemistry Chinese Academy of Sciences, Beijing 100190, China.

University of Chinese Academy of Sciences, Beijing 100049, China.

E-mail addresses: mengxw@mail.ipc.ac.cn

^c Department of Radiology, The First Affiliated Hospital of China Medical University, Shenyang 110001, China.

^d Department of Interventional Ultrasound, Chinese PLA General Hospital, Beijing 100853, China. E-mail: liangping301@hotmail.com

Calculation of the MW-thermo conversion efficiency

The MW-thermo conversion efficiency was calculated according to our previous work as follows:

Firstly, based on conservation of energy for the system:

$$Q_{input} \cdot \eta = Q_{output} = Q_{heat} + Q_{loss} \quad (1)$$

$$Q_{input} = p \cdot s_0 \cdot (t_n - t_0) \quad (2)$$

Q_{heat}

$$= \sum_{t=t_0}^{t=t_n} C_{solution} \cdot m \cdot \Delta T = C_{solution} \cdot m \cdot (T_1 - T_0) + C_{solution} \cdot m \cdot (T_2 - T_1) + \dots + C_{solution} \cdot m \cdot (T_n - T_{n-1})$$

$$= C_{solution} \cdot m \cdot (T_n - T_0) \quad (3)$$

Assumption ①: $T_{Env} \equiv T_0$ (4)

$$Q_{loss} = \sum_{t=t_0}^{t=t_n} u \cdot s_0 \cdot \Delta(T_{ZrMOF} - T_{Env}) \cdot \Delta t$$

$$= \sum_{t=t_0}^{t=t_n} u \cdot s_0 \cdot \Delta(f_1(t) - f_2(t)) \cdot \Delta t \quad (5)$$

Assumption ②: $\lim \Delta t = \lim(t_n - t_{n-1}) = dt \rightarrow 0^+$ (6)

$$\Delta(f_1(t) - f_2(t)) \cdot \Delta t = \sum_{t=t_0}^{t=t_n} [f_1(t) - f_2(t)] dt$$

$$= \int_{t_0}^{t_n} [f_1(t) - f_2(t)] dt = \Delta S \quad (7)$$

$$Q_{loss} = u \cdot s_0 \cdot \Delta S \quad (8)$$

Then $u \cdot s_0$ was calculated as follows:

$$\sum_{t=t_0}^{t=t_n} C_{solution} \cdot m \cdot \frac{dT}{dt} = -u \cdot s_0 \cdot \Delta T \quad (9)$$

θ was introduced: $\theta = \frac{\Delta T}{T_{max}}$ (10)

$$\sum_{t=t_0}^{t=t_n} C_{solution} \cdot m \cdot \frac{d\theta}{dt} = -u \cdot s_0 \cdot \theta \quad (11)$$

$$dt = - \frac{\sum_{t=t_0}^{t=t_n} C_{solution} \cdot m}{u \cdot s_0} \cdot \frac{d\theta}{\theta} \quad (12)$$

$$\xi \text{ was introduced: } \xi = \frac{\sum_{t=t_0}^{t=t_n} C_{solution} \cdot m}{u \cdot s_0} \quad (13)$$

$$t = \xi \cdot (-\ln \theta) + a \quad (14)$$

Finally, MW-thermo conversion efficiency (η) of ZrMOF NCs was calculated by the following equation:

η

$$\eta = \frac{\left[\sum_{t=t_0}^{t=t_n} C_{solution} \cdot m \cdot \Delta T + Q_{loss} \right]}{Q_{input}} = \left[C_{solution} \cdot m \cdot (T_n - T_0) + \frac{\sum_{t=t_0}^{t=t_n} C_{solution} \cdot m}{\xi_s} \cdot \int_{t_0}^{t_n} [f_1] \right]$$

- m (g): Total mass of the solution and ZrMOF NCs
- ΔT (K): Temperature change of the system
- Q_{input} (J): Electromagnetic energy of MW radiation
- Q_{heat} (J): Thermal energy of the solution containing ZrMOF NCs
- Q_{loss} (J): Lost of Thermal energy to the surroundings
- η : MW-thermo conversion efficiency of ZrMOF NCs
- P (W/cm²): Power of MW irradiation
- S_0 (cm²): Heating surface area of the container
- T_0 (K): Initial temperature before MW irradiation
- T_n (K): Highest temperature of the steady state
- u (W/(m²·K)): Heat transfer coefficient of the natural convection
- T_{ZrMOF} (K): Temperature of the solution containing ZrMOF NCs
- T_{Env} (K): Ambient surrounding temperature
- $f_1(t)$ and $f_2(t)$: Function formula of T_{ZrMOF} and T_{Env} for time

Table S1. Parameters for calculating MW-thermo conversion efficiency η of ZrMOF NCs dispersed in three solutions (water, 0.9 wt.% NaCl solution and DMEM).

Sample	$\sum c \cdot m \cdot \Delta T$ (J)	ξ_s	Q_{loss}	Q_{input}	η
			(J)	(J)	(%)
Water	3.73	445.36	65.04	2165.11	3.2 ± 0.4
NaCl	61.82	88.67	437.90	2165.11	23.1 ± 0.9
DMEM	87.30	70.13	553.59	2165.11	29.6 ± 0.7
ZrMOF in Water	5.49	427.14	71.69	2165.11	3.6 ± 0.6
ZrMOF in NaCl	90.74	72.45	529.30	2165.11	28.6 ± 0.9
ZrMOF in	113.17	65.79	679.80	2165.11	36.6 ± 0.9

DOX loading and pH-controlled release test

Standard calibration curve (the correlation coefficient was 0.99821) was as follows:

$$y = 0.05531 + 0.02045 \times x$$

y represents the absorption intensity of DOX at the wavelength of 483 nm, and x represents the corresponding concentration of DOX ($\mu\text{g/mL}$). And the loading rate of DOX-loaded ZrMOF-PEG-TPP (R_{loading}), the encapsulation efficiency of DOX ($R_{\text{encapsulation}}$) and the release rate of DOX-loaded ZrMOF-PEG-TPP (R_{release}) were calculated as follows, respectively:

$$R_{\text{loading}} = \frac{m_{\text{DOX}}'}{m_{\text{ZrMOF-PEG-TPP}} + m_{\text{DOX}}'} \quad (1)$$

$$R_{\text{encapsulation}} = \frac{m_{\text{DOX}}'}{m_{\text{DOX}}^0} \quad (2)$$

$$R_{\text{release}} = \frac{m_{\text{DOX}}''}{m_{\text{DOX}}'} \quad (3)$$

$m_{\text{ZrMOF-PEG-TPP}}$ represents the amount of ZrMOF-PEG-TPP NCs; m_{DOX}^0 was amount of DOX added in ZrMOF-PEG-TPP@DOX; m_{DOX}' and m_{DOX}'' represent loading capacity and release amount of DOX on ZrMOF-PEG-TPP@DOX NCs, respectively.

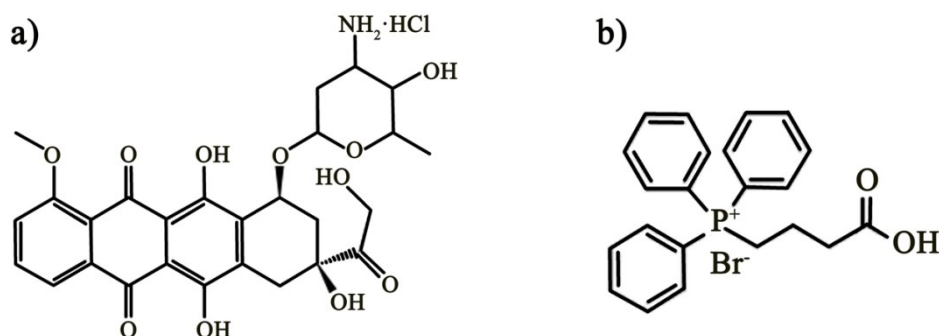


Fig. S1 The molecular structures of a) doxorubicin hydrochloride (DOX) and b) 3-Carboxypropyl triphenylphosphonium bromide (TPP).

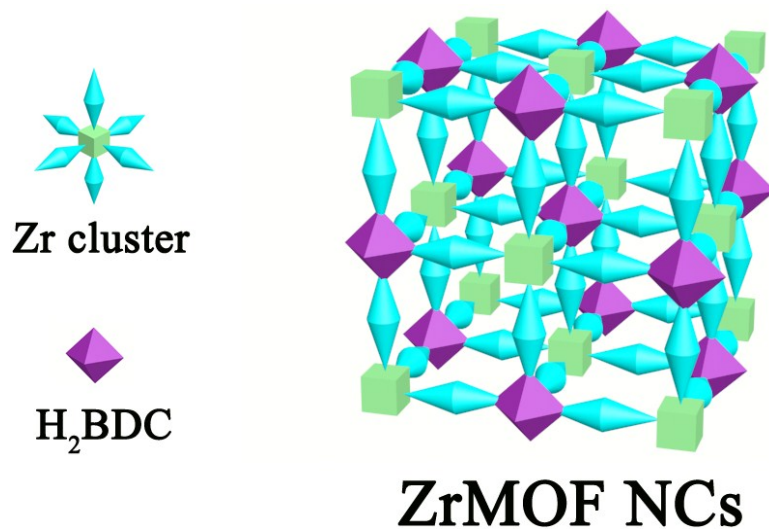


Fig. S2 The crystal structure of ZrMOF NCs. Zr cluster represents the inner $Zr_6O_4(OH)_4$ core of ZrMOF NCs.

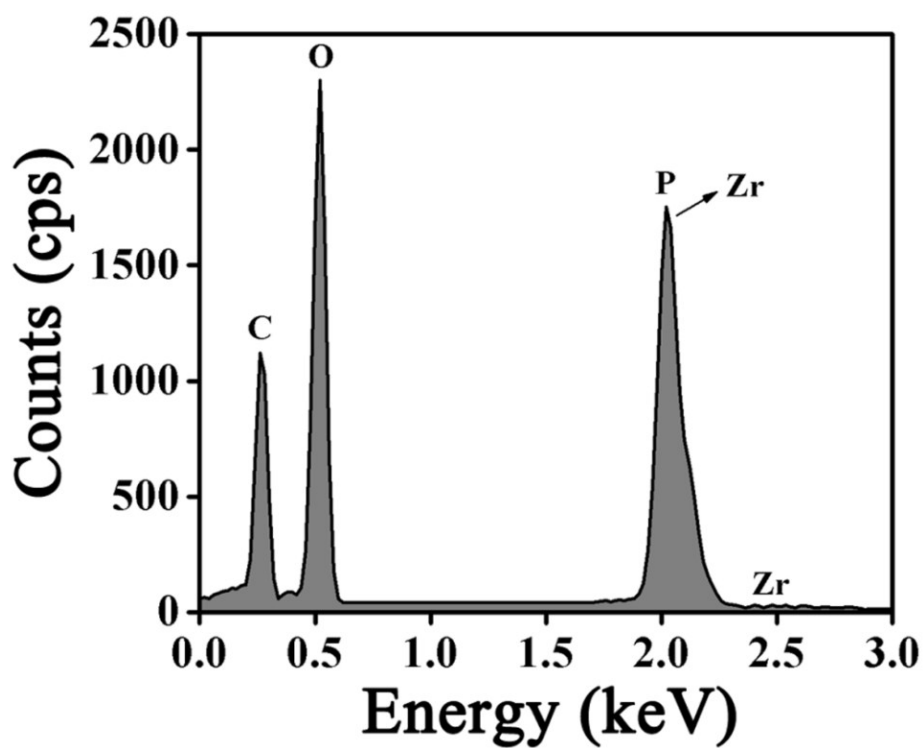


Fig. S3 Energy dispersive spectrum of ZrMOF-PEG-TPP NCs.

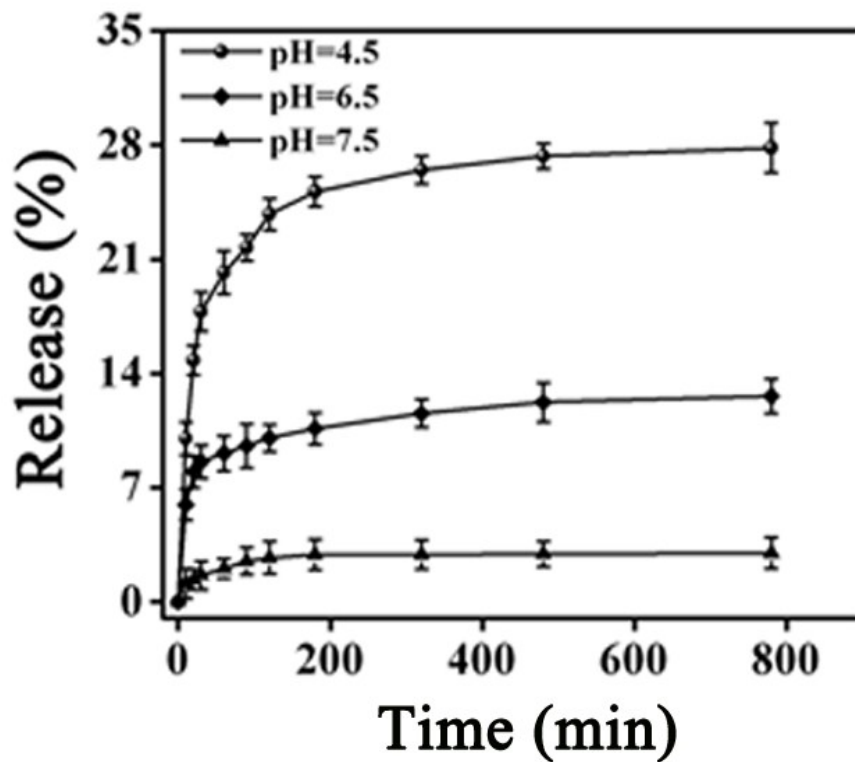


Fig. S4 pH-controlled release curves of ZrMOF-PEG-TPP@DOX NCs in different pH of PBS with time.

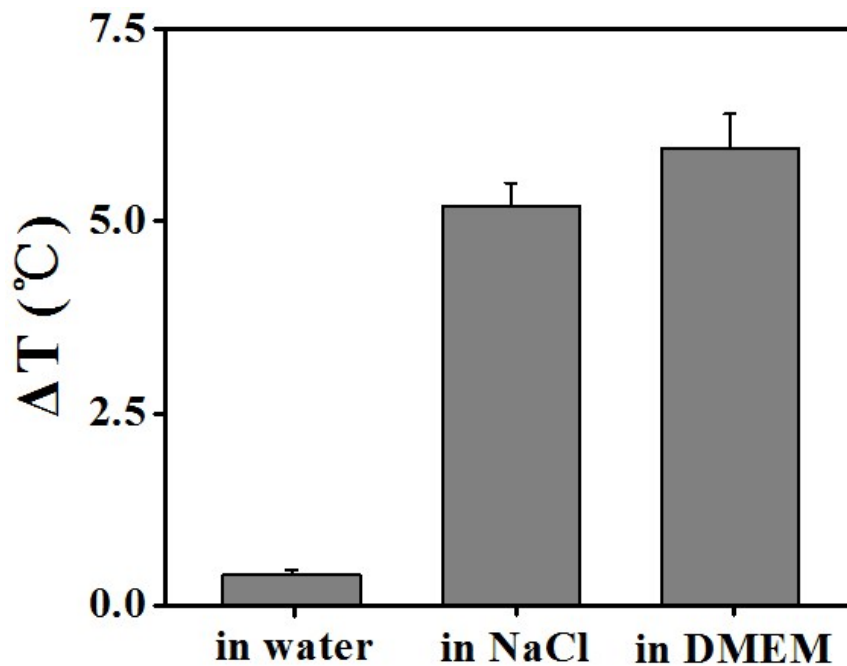


Fig. S5 The temperature change between water, 0.9 wt. % NaCl solution, DMEM and ZrMOF NCs dispersed in water, 0.9 wt. % NaCl solution and DMEM (10 mg/mL, 1.8 W/cm², 5 min), respectively.

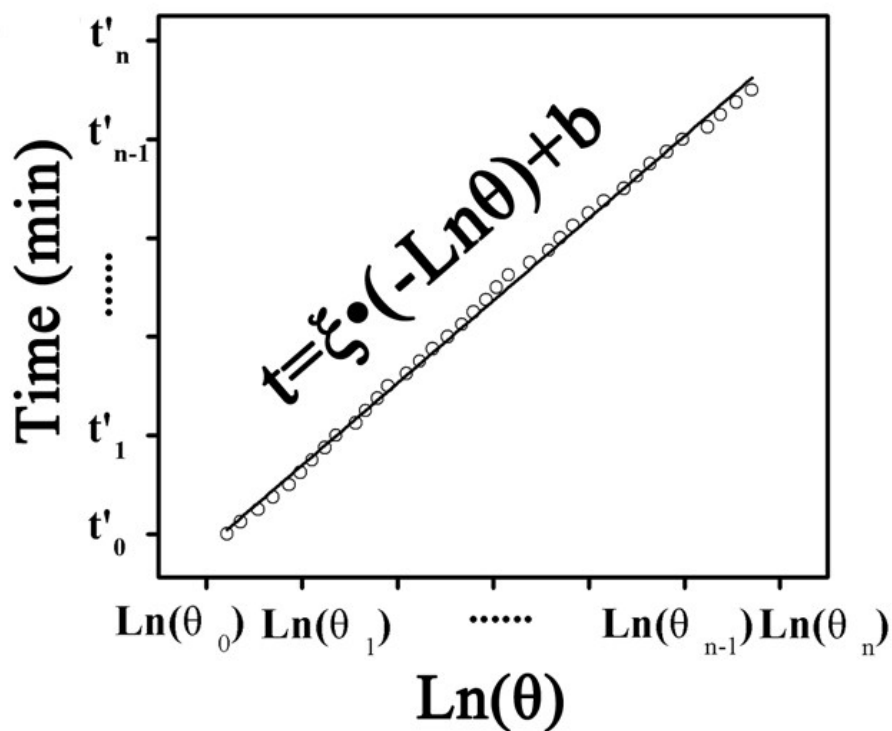


Fig. S6 The linear fitting of cooling curve for ZrMOF NCs accordingly.

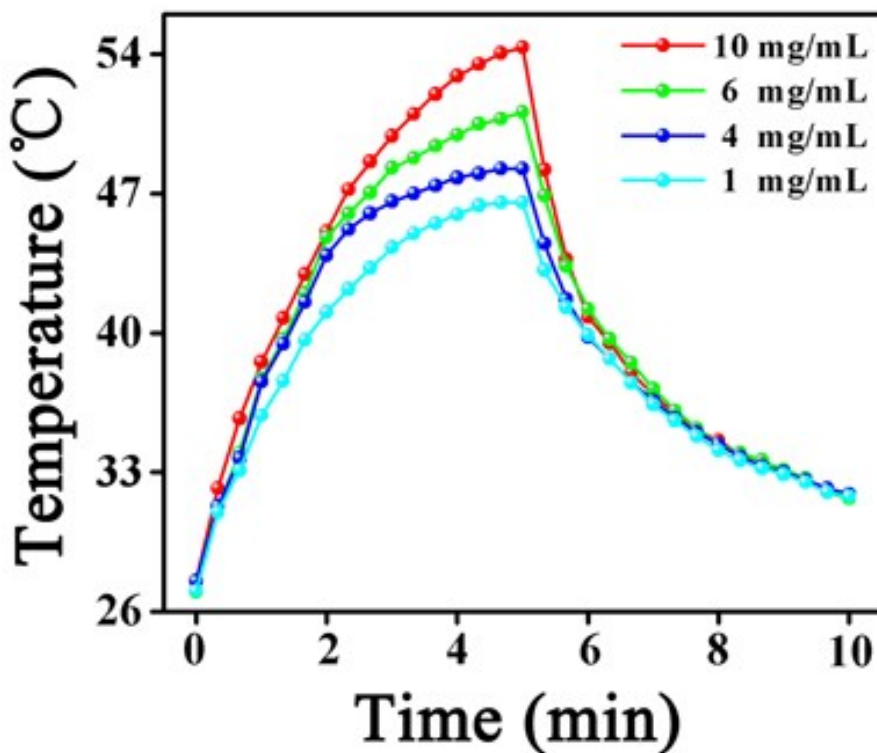


Fig. S7 At different concentrations of ZrMOF NCs (1.8 W/cm^2), the heating curves of ZrMOF NCs dispersed in DMEM under MW irradiation (5 min).

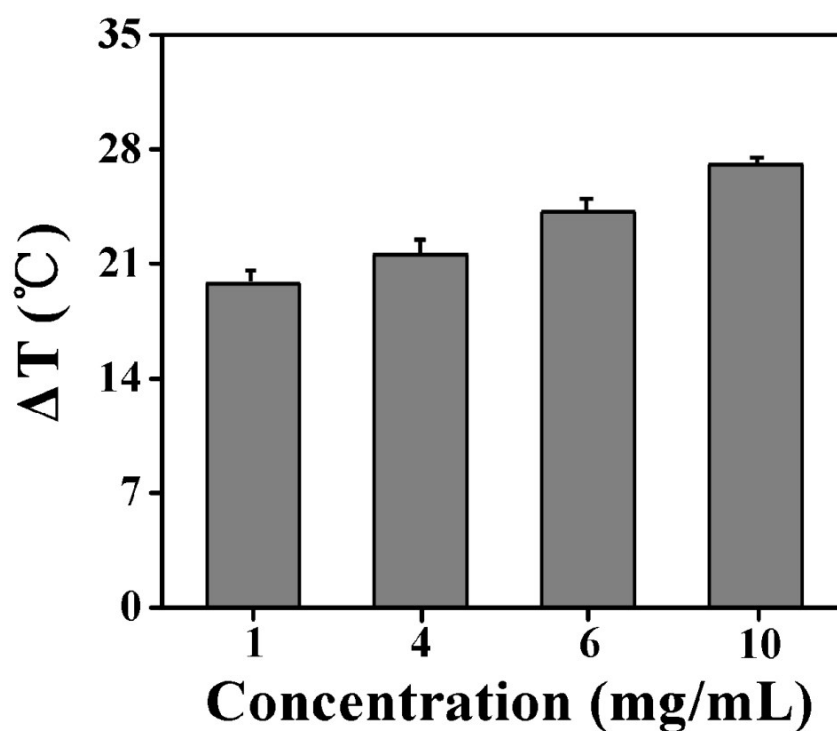


Fig. S8 The temperature changes of ZrMOF NCs dispersed in DMEM at the concentration of 1, 4, 6 and 10 mg/mL (1.8 W/cm², 5min).

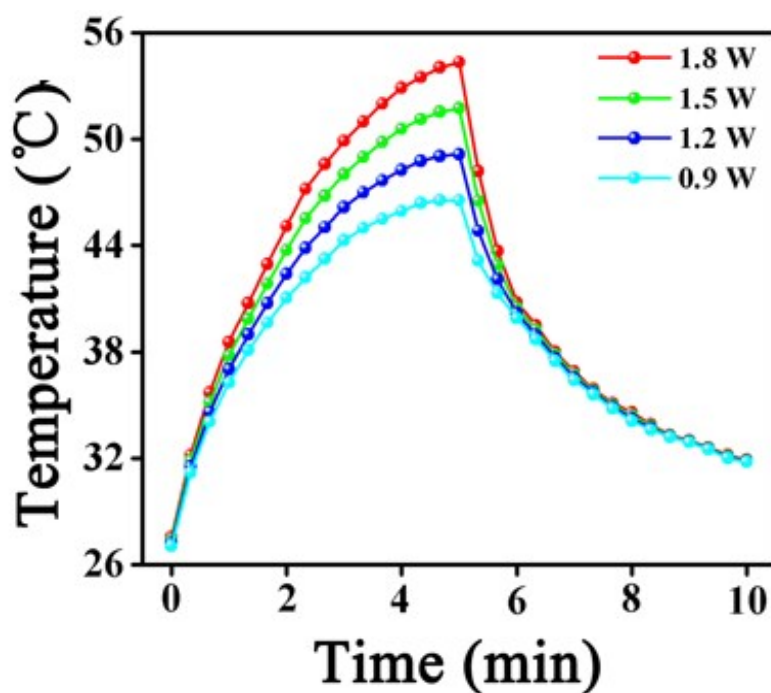


Fig. S9 At different MW irradiation powers of ZrMOF NCs (10 mg/mL), the heating curves of ZrMOF NCs dispersed in DMEM under MW irradiation (5 min).

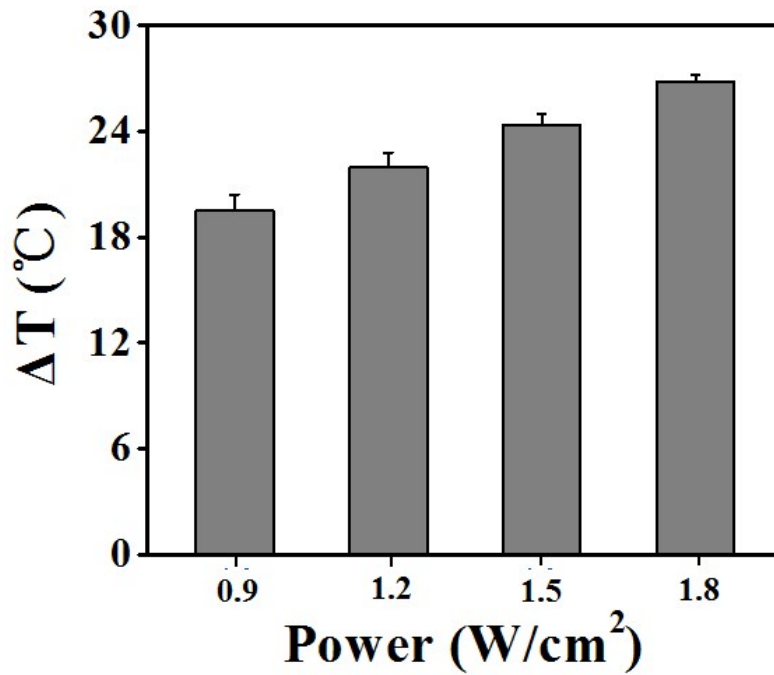


Fig. S10 The temperature changes of ZrMOF NCs dispersed in DMEM at the MW irradiation power of 0.9, 1.2, 1.5 and 1.8 W/cm² (10 mg/mL, 5 min).

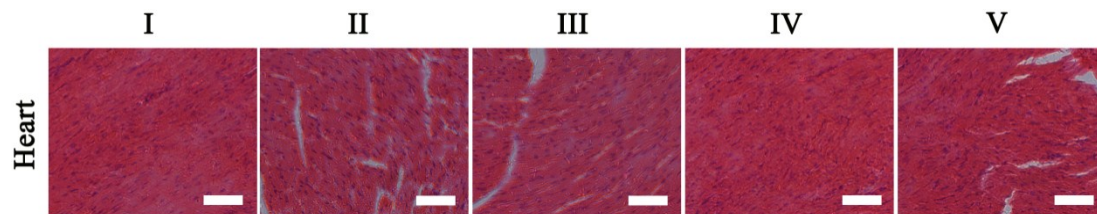


Fig. S11 H&E stained images of the heart in the mice with different treatments. I, II, III, IV and V was 5 wt.% glucose solution, MW, ZrMOF-PEG-TPP@DOX NCs, ZrMOF-PEG@DOX NCs + MW and ZrMOF-PEG-TPP@DOX NCs + MW groups, respectively. And the scale bar was 25 μm.

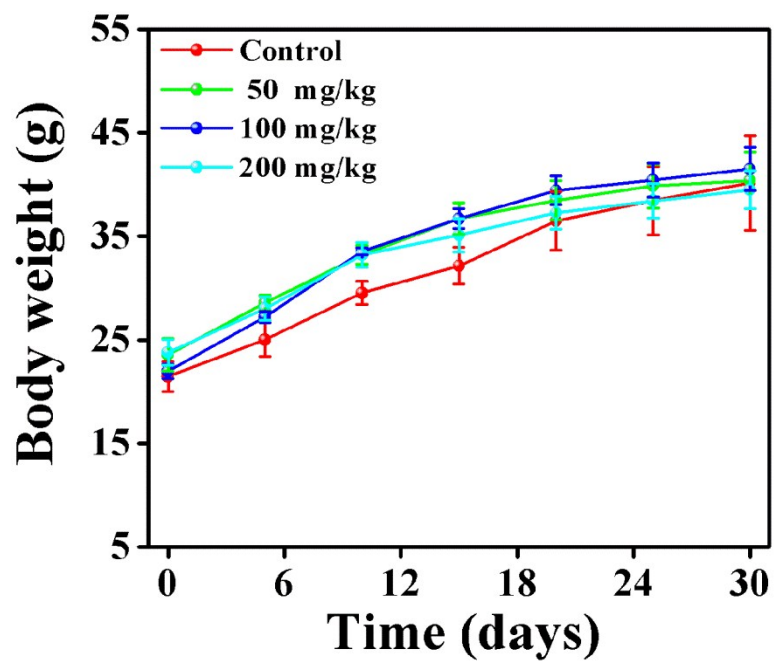


Fig. S12 The body weight changes of normal mice intravenously injected with ZrMOF-PEG-TPP@DOX NCs at the concentrations of 50, 100 and 200 mg/kg.

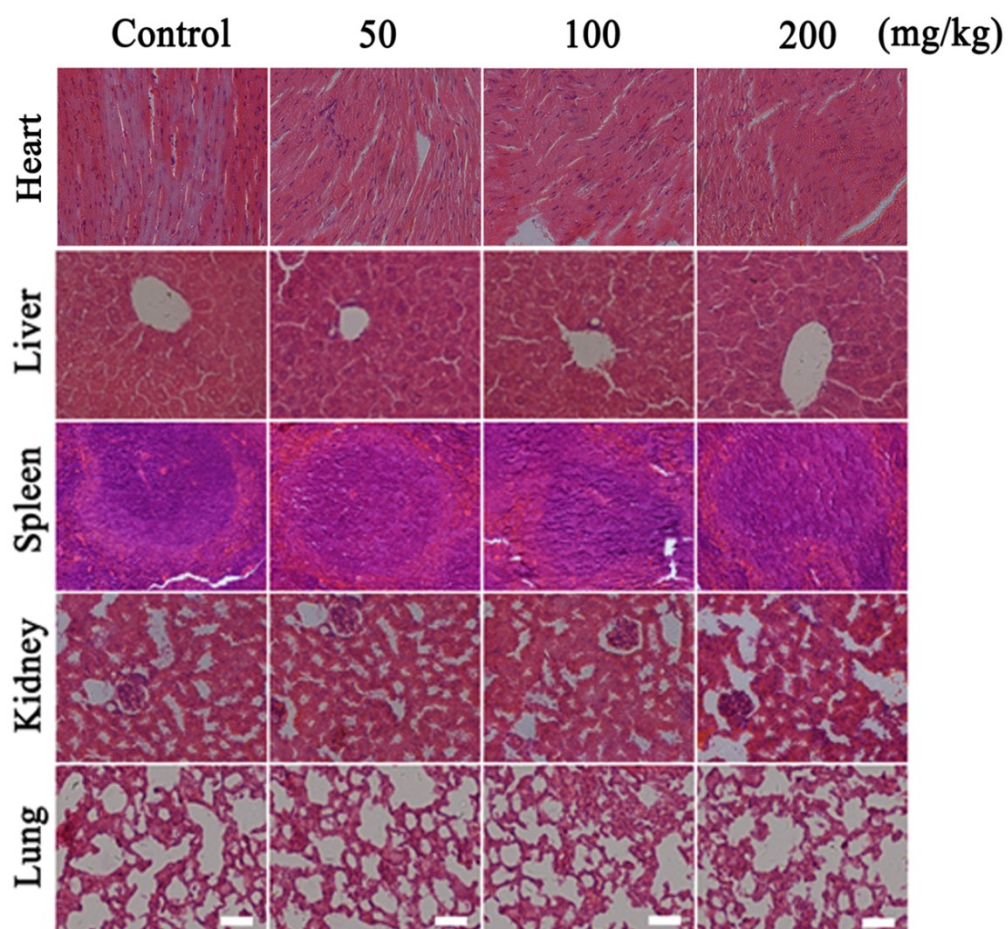


Fig. S13 H&E stained images of normal mice intravenously injected with ZrMOF-PEG-TPP@DOX NCs at the concentrations of 50, 100 and 200 mg/kg. And the scale bar was 25 μ m.